

Methods for enhancing the thermal durability of high-temperature
thermoelectric materials

Gunstein Skomedal, Nils R. Kristiansen, Marianne Engvoll
and Hugh Middleton

University of Agder
Faculty of Engineering and Science

and
Tegma AS, Kristiansand

This is the author's version of an article published in the journal:
Journal of Electronic Materials (2013)

DOI: 10.1007/s11664-013-2917-0

Methods for enhancing thermal durability of high-temperature thermoelectric materials

Authors: Gunstein Skomedal¹, Nils R. Kristiansen¹, Marianne Engvoll², Hugh Middleton¹⁸⁰¹

1) University of Agder, Norway

2) Tegma AS

Contact information: Email: gunstein.skomedal@uia.no, Telephone: +4791113267

Abstract: Thermoelectric materials such as Skutterudites and Magnesium Silicides are being investigated as promising alternatives for medium to high temperature waste heat recovery in the transport sector and industry. A critical success factor for the thermoelectric material is its stability over time when exposed to rapid heating and cooling during its lifetime. In this work the different degradation issues at high temperature are examined for these thermoelectric materials, and several means of enhancing durability have been evaluated. Initial thermal durability studies have been performed with Skutterudites and Magnesium Silicides with candidate coatings for protecting the materials from oxidation and sublimation during thermal cycles in air for up to 500 hours and up to 873K. The samples were then characterized by SEM and EDS. The results showed that it is possible to decrease degradation of the thermoelectric material without compromising the overall thermoelectric efficiency.

Keywords: skutterudite, Magnesiumsilicide, oxidation, durability, coating

Introduction:

The global energy consumption is increasing rapidly. Better ways to produce and utilize this energy is needed for a sustainable future. A large portion, > 60%, of the energy already produced is lost as heat [1]. Thermoelectric Generators are a good alternative for heat recovery in transport and process industry sector where large temperature gradients are available and space sometimes could be limited so that other heat recovery technologies cannot be used. Several good thermoelectric (TE) materials exist today that can exploit this potential [2], such as PbTe and TAGS, but price, production complexity and environmental issues amongst others have stopped these materials entering the civilian market on a large industrial scale.

Skutterudite, CoSb₃, (SKD) is one material that has received considerable attention over the last decade due to its relatively high ZT-values above 1 [3, 4] in the medium to high temperature range, 250-650°C. Magnesiumsilicide-based alloys (MGS) have also shown very good ZT-values above 1 in this temperature range [5]. MGS can be made from cheap, abundant and non-toxic raw materials and are very light compared to other well-known TE-materials.

Some of the main challenges with these materials are oxidation and sublimation of the substrate which reduces the lifetime of the TE-material. For SKD the oxidation and sublimation are well known and have been studied thoroughly over the last decade [6-12]. Already at 380°C oxidation starts forming a two layer structure of Sb₂O₃/Sb₂O₄ on the outside and CoSb₂O₄/CoSb₂O₆ on the inside. At temperatures up to about 600°C both layers are fairly stable and continue to grow following a parabolic rate law typical for diffusion controlled process with opposing diffusion of Sb outwards and O inwards. When the inner layer reaches a certain thickness it will split up into two distinct layers of CoSb₂O₆ and CoSb₂O₄. At higher temperatures the relatively high vapor pressures of the antimony oxides will cause them to evaporate faster than the bulk material can be oxidized and therefore a weight loss is observed. The antimony oxide layer is also

very brittle and tends to form a scale which spalls off the surface when it reaches a critical thickness further enhancing the degradation.

For MGS there are a wide variety of different alloys, for example the solid solution Mg₂Si_{1-x}Sn_x, and so the oxidation and sublimation behavior of such species is related to the particular composition of the material. There is relatively little published literature on this field to date but some examination of pure Mg₂Si has been carried out [13, 14]. TGA measurements showed that Mg₂Si will remain unreacted in air up to 450-500°C, but above these temperatures Mg₂Si reacts with O₂ to form MgO and Si. This is also a diffusion controlled reaction and it is therefore important to limit the O₂ flow towards the surface of the bulk material. Recent studies on Mg₂Si_{1-x}Sn_x using temperature dependent X-ray diffraction shows that it will start to decompose in air at temperatures as low as 400°C [15]. MgO, Si, Sn and other Mg₂Si_{1-x}Sn_x solid solutions will segregate out as separate phases on the surface of the bulk material and form a porous layer which does not hinder further oxidation and decomposition.

It is clear that to be able to adapt both SKD and MGS in TEG's at higher temperatures (>350-400°C) some form of protection against oxidation and sublimation is needed. One method which is widely used in thermoelectric modules is the full encapsulation of the modules and also filled with inert gas such as argon. Alternatively an aerogel can be casted around the whole leg assembly [16, 17] as it also will decrease parasitic heat losses. This module-level protection does on the other hand require more material in addition to TE-material adding to the total cost of the module. It is also fairly vulnerable to mechanical damage. Lastly, even if oxidation is hindered, a module-level protection is not sufficient to prevent sublimation on the surface of the TE-material. Since a module is made out of several TE legs connected in series, a leg-level protection could offer advantages with respect to price and simplicity of module design and assembly and at the same time hinder both oxidation and sublimation. This could be done by adding a protective layer during leg production.

Already several coating alternatives for leg-level protection have been evaluated for the use on SKD ranging

from thin metal layers to thicker composite glass coatings [18-25]. The most important properties of a coating, aside from hindering oxidation and sublimation of the TE-material, should be low electrical and thermal conductivity, matching thermal expansion with the TE-material, good adhesion to the substrate and to be chemically inert. It should also be applied by a cheap and reliable deposition method which could be readily adapted in the mass-production of legs.

In this work the thermal stability and degradation of CoSb_3 and $\text{Mg}_2\text{S}_{1-x}\text{Sn}_x$ have been evaluated along with candidate coatings for protection of the side surface of the TE-legs in a module. The coatings have been tested in both aging as well as thermal cycling set-ups in air.

Methods and Materials

For the studies on SKD materials, undoped Skutterudite, CoSb_3 , supplied by TEGma AS, were cut into cubes of 2.94^3 mm^3 . The samples used for the coating tests were as-cut, while the samples used for the oxidation tests were further polished with $1 \mu\text{m}$ diamond suspension. For experiments on Magnesiumsilicide compounds $\text{Mg}_2(\text{Si}_{0.4}\text{Sn}_{0.6})_{0.99}\text{Sb}_{0.01}$ produced at the Ioffe Institute through the ThermoMag program were used. Likewise the samples were polished using $1 \mu\text{m}$ diamond suspension. Oxidation experiments were conducted in a Lenton LTF 16/50/180 tube furnace with air-flow through the tube during thermal aging at 550°C , 600°C and 650°C for SKD and 350°C , 370°C and 400°C for MGS. The weight change of the samples were noted for aging times between 1 and 333h for SKD and 1-48h for MGS. Changes in surface structure were noted during the aging process. Several different types of coatings were applied on the samples. These could be grouped into different oxide/metal coatings, Boron Nitride, Silicone-Zn and also several glass ceramic coatings.

A small tube furnace optimized for running with faster heating/cooling rates was used for the thermal cycling experiments. Two rows of six SKD samples, both coated and uncoated, were fastened between two 1mm thick titanium plates (see figure 1) and placed inside a quartz tube located in the centre of the furnace in the uniformly heated zone. Titanium were chosen as the clamp material because of a good CTE-match (9 versus 10-11 for SKD). The furnace was then run in cycles between 200°C and 600°C with a dwell time at 600°C of 1h and ramp rates of $10^\circ\text{C}/\text{min}$. The experiment lasted for a total of 180 cycles in 500h. All samples from both aging and thermal cycling experiments were analysed using a JEOL SEM 6400 with EDAX both on surface and cross sections of the samples to identify reaction products.

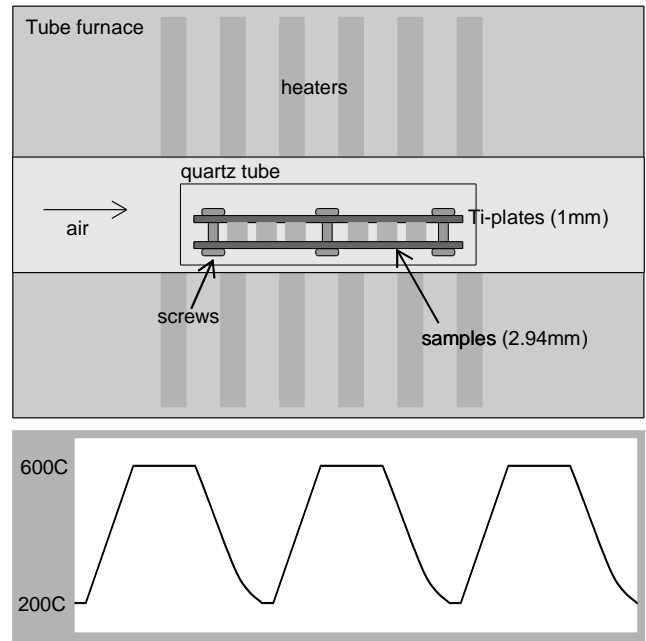


Fig. 1 Experimental set-up for thermal cycling experiments of CoSb_3

Results & Discussion

Oxidation of CoSb_3

An example of the oxidation of CoSb_3 can be seen in figure 2. The oxide forms two distinct layers of an outer $\text{Sb}_2\text{O}_3/\text{Sb}_2\text{O}_4$ layer and an inner $\text{CoSb}_2\text{O}_4/\text{CoSb}_2\text{O}_6$ layer. It was difficult to identify the cobalt antimony oxides in two separate layers, instead a more gradual decrease in O-content as a function of distance from outer surface can be seen.

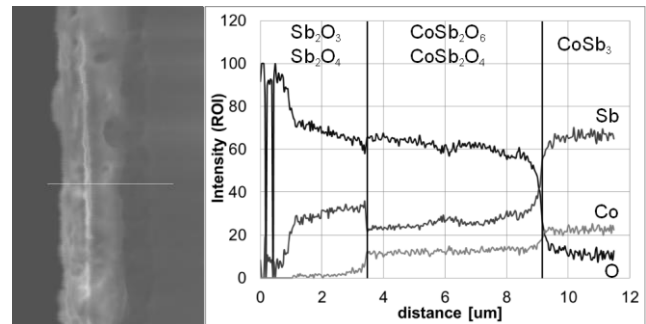


Fig. 2 Cross section of oxidized surface CoSb_3 after aging in air at 550°C for 24h

The weight change curves of the oxidation of the SKD material can be found in figure 3. At 550°C the oxidation of SKD follow a parabolic rate law in agreement with [9] and [10]; $(\Delta m)^2 = k_p t$, where Δm is the change in mass per unit area and k_p the parabolic rate constant. The two different stages described in [10] can also be seen with a slight drop in mass between possibly caused by scaling off of the outer oxide layers. The first stage has a slightly higher parabolic rate constant than the second with 5.6×10^{-6} and $2.1 \times 10^{-6} \text{ kg}^2\text{m}^{-4}\text{h}^{-1}$ respectively. Both of these values are two order of magnitude lower than found in [9]. This could be caused by a more coarse grain structure

which would slow down the diffusion of both oxygen and antimony. At 600°C and 650°C a weight loss is observed. According to [10] an increase in oxidation rate is found at 583°C which could be linked to the phase transition from α - Sb_2O_3 to β - Sb_2O_3 and subsequent increase in evaporation which would then be faster than the oxidation process resulting in a net mass loss.

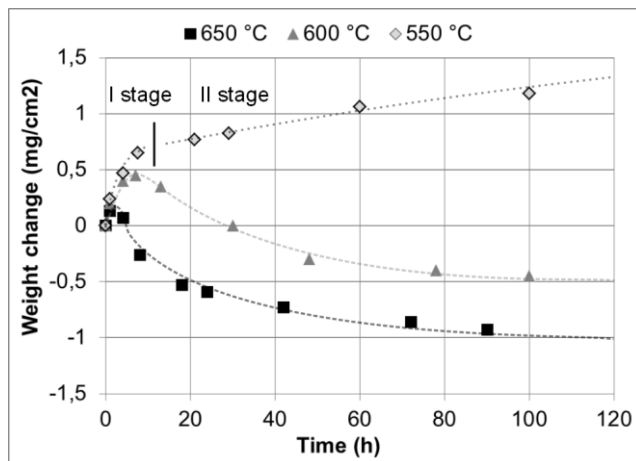


Fig. 3 Weight change of bulk CoSb_3 in air as a function of time and aging temperature. Dotted lines included for illustration only

Coatings & thermal cycling of CoSb_3

Most of the candidate coatings tested showed little to no protection against oxidation and sublimation of SKD. The oxide coatings, silicone-Zn coating and glass ceramic coatings were found to be either too porous or did not adhere to the SKD surface sufficiently. The only coating product that hindered the formation of the oxidation layer and simultaneously possessed good mechanical stability was an oxide/metal coating mostly containing Al_2O_3 as seen in figure 4. The oxide layer was reduced in thickness from 15-20 μm for the uncoated sample to around 3.5 μm for the coated sample. No pure Sb_2O_4 layers formed, but instead the Sb diffused into the coating. The CoSb_2O_4 oxide had good adhesion to the unoxidized CoSb_3 thus avoiding the formation of the CoSb_2O_6 and Sb_2O_4 layers making the oxide layer much more mechanically stable. This allowed the coating to remain adhered to the sample. The same coating was used on a sample during thermal cycling. In figure 5 it can be seen that the coating almost eliminated oxidation completely, only a very thin intermediate layer of around 1.5 μm formed after 180cycles up to 600°C, totaling over 180h at this temperature. Uncoated samples had oxide layers of around 20 μm which shows that the coating effectively hindered both sublimation of Sb and oxidation of the bulk material. Another very important observation is that the coating layer becomes fully oxidized and both thermal losses and electrical conduction are kept to a minimum. Some cracks were observed between the substrate and the coating. This was most probably a result of sample preparation since no enhanced oxidation is seen on places where visible cracks appear. It was also found that a thinner layer generally will be more mechanically stable than thicker layers during thermal cycling. This could be seen on samples with

thicker coating layers where oxidation layers up to 10 μm where found.

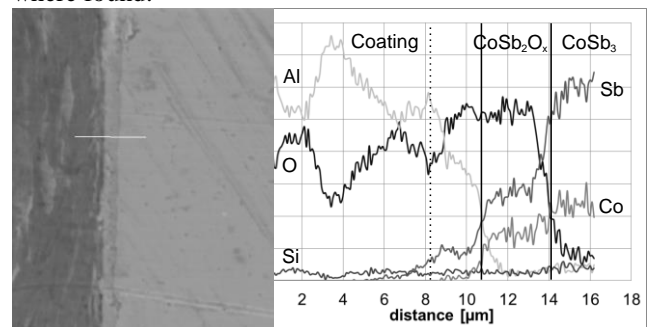


Fig. 4 Cross section of SKD with Al-O coating after aging at 600°C in air for 48h. The coating have decreased the oxidation of the SKD surface and hindered sublimation of Sb

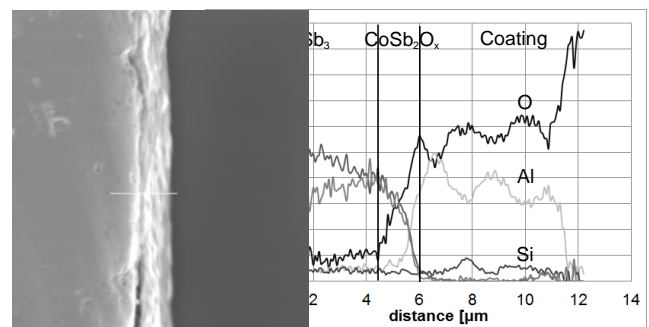


Fig. 5 Cross section view of SKD with Al_2O_3 coating after 180cycles up to 600°C. The thin coating layer (~6 μm) seems to almost eliminate all oxidation of the SKD, only a thin layer about 1.5 μm thick of oxide $\text{CoSb}_2\text{O}_4/\text{CoSb}_2\text{O}_6$ with a gradual transition into the coating layer can be seen

A cross section view of an SKD sample coated with BN after 180 cycles up to 600°C can be seen in figure 6. In this special case the oxide layer is 3 times thicker (65-70 μm) than even for uncoated samples. It is unclear whether this apparent increase in oxidation rate is a result of the BN-coating acting as a catalyst increasing the oxidation rate, or that the uncoated samples actually had the same oxidation rate but that the outer oxide layers had evaporated so they were not found in the cross sectional analysis. This is also what can be seen in figure 3 where mass loss is observed for samples exposed to temperatures above 600°C. The BN coating is too porous to stop oxygen transport through the coating, but could still be dense enough to avoid sublimation and scaling off of the outer oxide layers. This effect needs to be studied further in order to understand the rate limiting steps in the oxidation of CoSb_3 and how this knowledge could be used to manipulate the reaction kinetics.

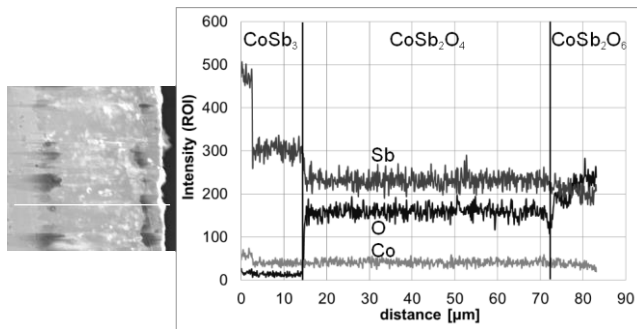


Fig. 6 Cross section view of SKD coating with BN after 180 cycles up to 600°C. The BN coating peeled off during demounting and preparation. A very thick oxide layer has formed of around 65-70μm

Oxidation and protection of Mg₂(Si-Sn)

No distinct oxidation layer was observed for the tested Mg₂Si_{0.4}Sn_{0.6} sample as with CoSb₃. As seen in figure 7 the material was slightly inhomogeneous and had some dark Si-rich regions with a composition approximating to Mg₂Si_{0.7}Sn_{0.3}.

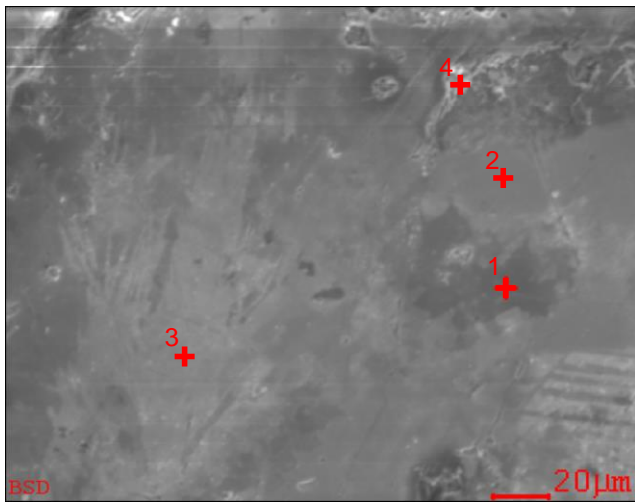


Fig. 7 Oxidized surface of Mg₂Si_{0.4}Sn_{0.6} after 48h at 370°C. Dark Si-rich regions show slightly lower MgO content than brighter Sn-rich regions. Point 4 is almost fully oxidized

Table 1: Atomic percentage of each elements present in point 1-4 in figure 7.

	Mg	Si	Sn	O	Original Phase
1	63,2	27,3	2,7	6,9	Mg ₂ Si _{0.9} Sn _{0.1}
2	53,0	6,3	14,0	26,7	Mg ₂ Si _{0.32} Sn _{0.68}
3	58,6	9,4	17,7	14,3	Mg ₂ Si _{0.35} Sn _{0.65}
4	44,6	2,6	4,3	48,6	Mg ₂ Si _{0.38} Sn _{0.62}
Avg	57,3	10,3	13,9	18,5	Mg ₂ Si _{0.43} Sn _{0.57}

After aging at 350°C for 24h very little oxidation was observed and only parts of the surface showed some increase in O content compared to room temperature. The sample heated for 48h at 370°C showed a slight increase in oxidation. SEM and EDS analysis (using an acceleration voltage of 15kV) of the surface facing the heat source showed a uniform layer of MgO with some Sn content, but no Si was seen in the uppermost layer. The other side of

the sample showed a more diversified oxidation related to the phase composition, as seen in figure 6 and table 1. A general observation was that the higher the Sn content of the original phase, the higher the oxygen content. In other words the Sn-rich phases decomposes much faster at lower temperatures than Si-rich phases. The mechanism for how the decomposition in air for Mg₂(Si-Sn) solid solution evolves needs to be studied further.

Two samples of MGS, one uncoated and one completely covered by the Al₂O₃ coating, were aged in air at 400°C for 24h. The uncoated samples showed a high rate of decomposition with one half of the sample completely oxidized as seen as a black MgO porous layer. The decomposition and oxidation seems to selfpropagate starting from one end of the sample and eating its way inwards. As the oxidation of Mg is highly exothermic this could readily explain this run away on oxidation rate. The porous structure disintegrated almost completely on handling and so was difficult to analyse. No sign of Sn and Si were found in the outer layers. The coated sample showed no sign of degradation at all, as seen in figure 8. It is evident that the coating needs to be very dense to avoid any oxygen reaching the surface. Further work is required to determine if the coating can work at higher temperatures than those studied here.

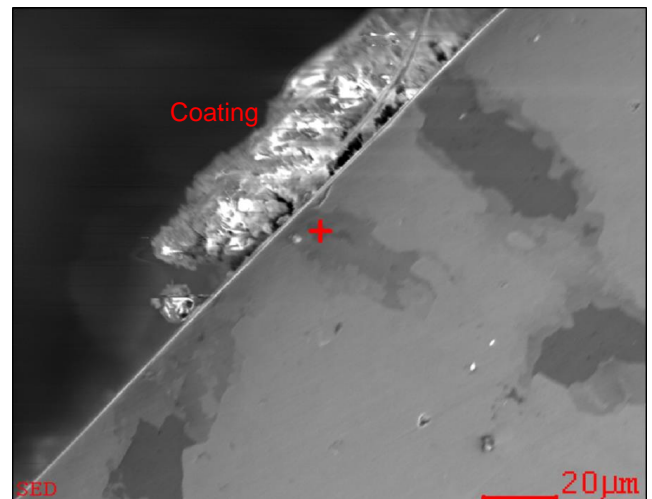


Fig. 8 Cross sectional view of Mg₂Si_{0.4}Sn_{0.6} covered with a Al₂O₃-coating after aging for 24h at 400°C. The sample showed no sign of degradation

Conclusion

Thermal durability studies in air on both pure CoSb₃ and Mg₂Si_{0.4}Sn_{0.6} have been conducted, along with the testing of different coatings to avoid degradation of the TE-material over time. Reaction kinetics and products of the oxidation of CoSb₃ have been confirmed. The oxide layers seemed also fairly stable during thermal cycling; no increase in oxidation rate was found as a result of cracking/scaling of the outer oxide layers. Although several coatings were tested only an Al₂O₃ coating was found to protect effectively from oxidation. After 180 cycles up to 600°C oxidation layers were decreased from

20 µm for uncoated samples, down to 1.5 µm for the coated samples. All the other coatings tested were either too porous, so O₂ and Sb diffusion was not hindered sufficiently, or didn't offer good adhesion. Moreover mechanical instability due to mismatch in CTE with the substrate resulted in cracks forming between coating and substrate.

Initial studies of the oxidation reactions of Mg₂(Si-Sn) solid solutions showed a dependency on the onset and speed of the oxidation as a function of increased Sn-content of the solid solution. Even at temperatures as low as 350 – 370°C Mg₂Si_{0.4}Sn_{0.6} will start to decompose into MgO, Sn, Si and other solid solutions of Mg₂Si_{1-x}Sn_x. At 400°C the reaction rate increases substantially and large black porous crystals of MgO grow rapidly out of the bulk material in a self-propagating manner because the oxidation of Mg is highly exothermic. Adding an Al₂O₃ coating at the same temperature caused the oxidation and decomposition to be effectively hindered. This coating is also believed to work at higher temperatures.

Acknowledgements

The authors wish to acknowledge financial support from the ThermoMag Project, which is co-funded by the European Commission in the 7th Framework program (contract NMP4-SL-2011-263207), by the European Space Agency and by the individual partner organizations.

References

- Library, L.L.N. *U.S. Energy Flow*. 2012 [cited 2013 25. October]; Available from: <https://flowcharts.llnl.gov/energy.html#2012>.
- Snyder, G.J. and E.S. Toberer, *NAT MATER*, 2008. **7**(2): p. 105.
- Alam, H. and S. Ramakrishna, *Nano Energy*, 2013. **2**(2): p. 190-212.
- Shi, X., J. Yang, J.R. Salvador, M. Chi, J.Y. Cho, H. Wang, S. Bai, J. Yang, W. Zhang, and L. Chen, *J AM CHEM SOC*, 2011. **133**(20): p. 7837-7846.
- Zaitsev, V.K., M.I. Fedorov, E.A. Gurieva, I.S. Eremin, P.P. Konstantinov, A.Y. Samunin, and M.V. Vedernikov, *PHYS REV B*, 2006. **74**(4): p. 045207.
- Hara, R., S. Inoue, H.T. Kaibe, and S. Sano, *J ALLOY COMPD*, 2003. **349**(1-2): p. 297-301.
- Leszczynski, J., A. Malecki, and K.T. Wojciechowski, *INT CONF THERMOELECT*, 2007.
- Godlewska, E., K. Zawadzka, A. Adamczyk, M. Mitoraj, and K. Mars, *OXID MET*, 2010. **74**(3-4): p. 113-124.
- Zhao, D., C. Tian, S. Tang, Y. Liu, and L. Chen, *J ALLOY COMPD*, 2010. **504**(2): p. 552-558.
- Leszczynski, J., K. Wojciechowski, and A. Malecki, *J THERM ANAL CALORIM*, 2011. **105**(1): p. 211-222.
- Zhao, D., C. Tian, Y. Liu, C. Zhan, and L. Chen, *J ALLOY COMPD*, 2011. **509**(6): p. 3166-3171.
- Xia, X., P. Qiu, X. Shi, X. Li, X. Huang, and L. Chen, *J ELECTRON MATER*, 2012. **41**(8): p. 2225-2231.
- Riffel, M. and J. Schilz, *INT CONF THERMOELECT*, 1997: p. 283-286.
- Tani, J.-i., M. Takahashi, and H. Kido, *J ALLOY COMPD*, 2009. **488**(1): p. 346-349.
- Bourgois, J., J. Tobola, L. Chaput, P. Zwolenski, D. Berthebaud, F. Gascoin, Q. Recour, and H. Scherrer, *Functional Material Letters : Frontier of Thermoelectrics*, (in press).
- Sakamoto, J.S., G.J. Snyder, T. Calliat, J.-P.S. Fleurial, M. Jones, and J.-A. Palk, *US 7,461,512 B2*, 9 Dec 2008
- Salvador, J., J. Cho, Z. Ye, J. Moczygemba, A. Thompson, J. Sharp, J. König, R. Maloney, T. Thompson, J. Sakamoto, H. Wang, A. Wereszczak, and G. Meisner, *J ELECTRON MATER*, 2012: p. 1-11.
- Saber, H.H. and M.S. El-Genk, *ENERG CONVERS MANAGE*, 2007. **48**(4): p. 1383-1400.
- Saber, H.H., M.S. El-Genk, and T. Caillat, *ENERG CONVERS MANAGE*, 2007. **48**(2): p. 555-567.
- Godlewska, E., K. Zawadzka, R. Gajerski, M. Mitoraj, and K. Mars, *Ceramic Materials*, 2010. **62**(4): p. 490-495.
- Godlewska, E., K. Zawadzka, K. Mars, R. Mania, K. Wojciechowski, and A. Opoka, *OXID MET*, 2010. **74**(3-4): p. 205-213.
- Wei, P., C.-L. Dong, W.-Y. Zhao, and Q.-J. Zhang, *J INORG MATER*, 2010. **25**(6): p. 577-582.
- Dong, H., X. Li, X. Huang, Y. Zhou, W. Jiang, and L. Chen, *CERAM INT*, 2012(0).
- Dong, H., X. Li, Y. Tang, J. Zou, X. Huang, Y. Zhou, W. Jiang, G.-j. Zhang, and L. Chen, *J ALLOY COMPD*, 2012. **527**(0): p. 247-251.
- Zawadzka, K., E. Godlewska, K. Mars, and M. Nocun, *AIP CONF PROC*, 2012. **1449**(1): p. 231-234.